Chin. Geogra. Sci. 2016 Vol. 26 No. 3 pp. 314–324
doi: 10.1007/s11769-016-0811-4

Springer Science Press
www.springerlink.com/content/1002-0063

Landform Planation Index Extracted from DEMs: A Case Study in Ordos Platform of China

QIAN Yeqing, XIONG Liyang, LI Jilong, TANG Guoan

(*Key Laboratory of Virtual Geographic Environment*, *Nanjing Normal University*, *Ministry of Education*, *Nanjing* 210023, *China*; *State Key Laboratory Cultivation Base of Geographical Environment Evolution*, *Nanjing* 210023, *China*; *Jiangsu Center for Collaborative Innovation in Geographical Information Resource Development and Application*, *Nanjing* 210023, *China*)

Abstract: Planation surface, a surface that is almost flat, is a kind of low-relief landforms. Planation surface is the consequence of the denudation and planation processes under a tectonic stable condition. The quantitative expression of the characteristics of planation surface plays a key role in reconstructing and describing the evolutionary process of landforms. In this study, Landform Planation Index (LPI), a new terrain derivative, was proposed to quantify the characteristics of planation surface. The LPIs were calculated based on the summit surfaces formed according to the clustering results of peaks. Ten typical areas in the Ordos Platform located in the central part of the Loess Plateau of China are chosen as the test areas for investigating their planation characteristics with the LPI. The experimental results indicate that the LPI can be effectively used to quantify the characteristics of planation surfaces. In addition, the LPI can be further used to depict the patterns of spatial differentiation in the Ordos Platform. Although the present Ordos Platform area is full of the high-density gullies, its planation characteristics is found to be well preserved. Furthermore, the characteristics of the planation surfaces can also reflect the original morphology of the Ordos Platform before the loess dusts deposition process evolved in this area. The statistical results of the LPI show that there is a gradually increasing tendency along with the increasing of slope gradient of summit surface. It indicates that the characteristics of planation surfaces vary among test areas with different landforms. These findings help to deepen the understanding of planation characteristics of the loess landform and its underlying paleotopography. Results of this study can be also served as an important theoretical reference value for revealing the evolutionary process of loess landform.

Keywords: Landform Planation Index (LPI); peak; summit surface; Digital Elevation Model (DEM); Ordos Platform, China

Citation: Qian Yeqing, Xiong Liyang, Li Jilong, Tang Guoan, 2016. Landform Planation Index extracted from DEMs: a case study in Ordos Platform of China. *Chinese Geographical Science*, 26(3): 314–324. doi: 10.1007/s11769-016-0811-4

1 Introduction

Planation surface is a kind of low-relief morphology of earth landforms, which should be the consequence of denudation and planation processes under a tectonic stable condition. The process of planation is one of the most important theoretical problems in the research of geomorphology (Cui *et al.*, 1999). The recognition and reconstruction of planation surface are the foundation for exploring planation processes and its underlying formation mechanism with landform analysis techniques. Traditional methods extracted the planation surfaces by manually delineating the planation boundaries on the topographical maps (Nash, 1988; Coltorti and Pieruccini, 2000; Feng and Cui, 2002). These manual methods, however, are time-consuming and error-prone, which are difficult to be applied for quantitative analysis of the characteristics of planation surfaces (Liu *et al.*, 1999).

With the development of Digital Elevation Model

Received date: 2015-07-27; accepted date: 2015-11-02
Foundation item: Under the auspices of National Natural Science Foundation of China (No. 41201464, 41471316), Priority Academic Program Development of Jiangsu Higher Education Institutions (No. 164320H101)
Corresponding author: XIONG Liyang. E-mail: xiongliyang@163.com

(DEM) applications and Geographic Information System (GIS) spatial analysis techniques (Bi *et al.*, 2006; Grohmann and Miliaresis, 2013; Tang, 2014), geomorphological analysis with the descriptive method (Evans, 1972; Veldkamp and Dijke, 2000) or field investigation method (Thorne, 1998; Poulos *et al.*, 2012) has been undergoing a rapid advancement in both concept and methodology. Digital terrain analysis has been used to calculate the basic terrain derivatives (e.g., slope, aspect) (Carbonel *et al.*, 2015; Rigol-Sanchez *et al.*, 2015), to reveal the spatial distribution of landform types (Dennis, 2004; Hara *et al*., 2008; Xiong *et al*., 2015), and to automatically extract the terrain features (e.g., peaks, saddles) (Lu *et al.*, 1998; Dinesh, 2007; Xiong *et al.*, 2013). There is a growing interest in automatic identification of the planation surfaces with DEMs. Zhang and Huang (1995) studied the planation surfaces in north Guangdong Province of China using a fuzzy model, which combines three standard factors of planation surface identification, including lithology, terrain and field survey. Dong and Tang (1997) developed a numerical model of the planation process in Qinghai-Tibet Plateau. Based on that model, the uplift and denude-planned alternating processes of Tibetan Plateau were reconstructed. Liu *et al.* (1999) extracted the planation surfaces of the Meiwu Plateau based on the geomorphological parameter system. Johansson (1999) constructed the absolute relief map and the trending height profiles based on DEMs. Coltorti and Pieruccini (2000) studied a late lower Pliocene planation surface across the Italian Peninsula by investigating the natural environment, geological age and later relationship of the remnants of planation surface. The constructed information was then used for identification and classification of the palaeotopography. Wu and Chen (2013) used an optimized windows analysis to find the distribution of relief degree and slope gradient of different height level. The distribution of the planation surfaces of the Yuntai Mountain was then analyzed based on information of the elevation, the slope gradient and the relief degree. Bessin *et al.* (2015) characterized and mapped the planation surfaces of the Armorican Massif based on a combination of three different GIS analysis methods (i.e., 3D visualization of the DEM, slope and curvature analysis from the DEM, and landform classifications from the DEM analysis).

Plenty of works have been done to reconstruct and recognize the planation surfaces (Yi *et al.*, 2000; Cui *et al.*, 2002; Römer, 2010; Li *et al.*, 2012; Wang *et al.*, 2012; Haider *et al.*, 2015). However, difficulties and challenges are still existing in this field. At present, there is a lack of a specific terrain index, which can be used to quantify the characteristics of the planation surfaces. Therefore, it is necessary to design a new geomorphological index to enable an unbiased identification of the planation surfaces. With the increasing maturity of terrain characteristics expression based on DEMs, it provides a new way to propose a terrain index to express and extract the planation surface on a basis of full consideration of the planation characteristics.

Unlike the planation characteristics of Tibetan Plateau (Cui *et al.*, 1996; 1997; Li *et al.*, 1996; Li and Fang, 1999; Zhang, 2008), the Ordos Platform in the Loess Plateau, China has inherent characteristics of planation. The underlying bedrock landform is largely originated from the planation surfaces of Ordos Platform. Currently, the bedrock terrain of the Ordos Platform is covered with the thick loess deposits. During the geomorphic evolution and the loess landform formation process, original Ordos planation surfaces have been buried by loess deposition process or even destroyed by the gully erosion on the top layer. However, the essential landform features of the Ordos Platform are still preserved (Xiong *et al*., 2014a). The geological background of the Ordos Platform has been undergoing integral and intermittent uplift movements during the Quaternary period. The current loess terrain can reflect the morphological variations of the underlying paleotopography. Therefore, the topographic relief relationship between current residual summit surfaces and original paleotopography tends to be uniform in general (Xiong *et al.*, 2014b). The planation characteristics of original underlying paleotopography could be represented by current summit surfaces during the loess deposition and accumulation process. Therefore, it is possible to explore the planation characteristics of loess landform and its underlying paleotopography in the Ordos Platform with the summit surfaces.

This study focuses on the identification of the planation surfaces from the morphological perspective. The planation surfaces are the geographical units with distinct morphological characteristics, which can be defined by the geomorphometric parameters derived from DEMs. The DEMs in different landform type are

adopted as the experimental data. Peaks are extracted from test areas with different landforms in the Ordos Platform, China. After that, the summit surfaces formed by the elevation connection of the cluster peaks are detected in different landform areas. At last, Landform Planation Index (LPI) based on the slope gradient and relative terrain relief of the summit surface is used for extracting and describing the characteristics of the planation surfaces.

2 Materials and Methods

2.1 Study area

The Ordos Platform (34°29′–40°29′N, 105°45′–111°56′E), located in the central part of the Loess Plateau with a total area of 257 062 km^2, is chosen as the study area. It contains the most severe soil erosion area in the Loess Plateau. The elevation of study area ranges from 364 to 2620 m. A semi-arid continental monsoon climate with average annual precipitation ranges from 200 to 500 mm exists in this area. Ten selected test areas are distributed from north to south in Ordos Platform. These test areas represent different landform types with their varied morphological characteristics. The distribution of test areas is shown in Fig. 1.

2.2 Data

The experimental data is the DEM with spatial resolution of 5 m, which is provided by Shaanxi Geomatics Center of National Administration of Surveying, Mapping and Geoinformation (http://www.sxgis.cn/). The geomorphologic division maps at the scale of 1∶10 000 is used as the reference data. The test areas are Shenmu, Yulin, Jingbian, Suide, Dingbian, Yanchuan, Ganquan, Yijun, Chunhua, and Fengxiang. Their landform parameters are shown in Table 1.

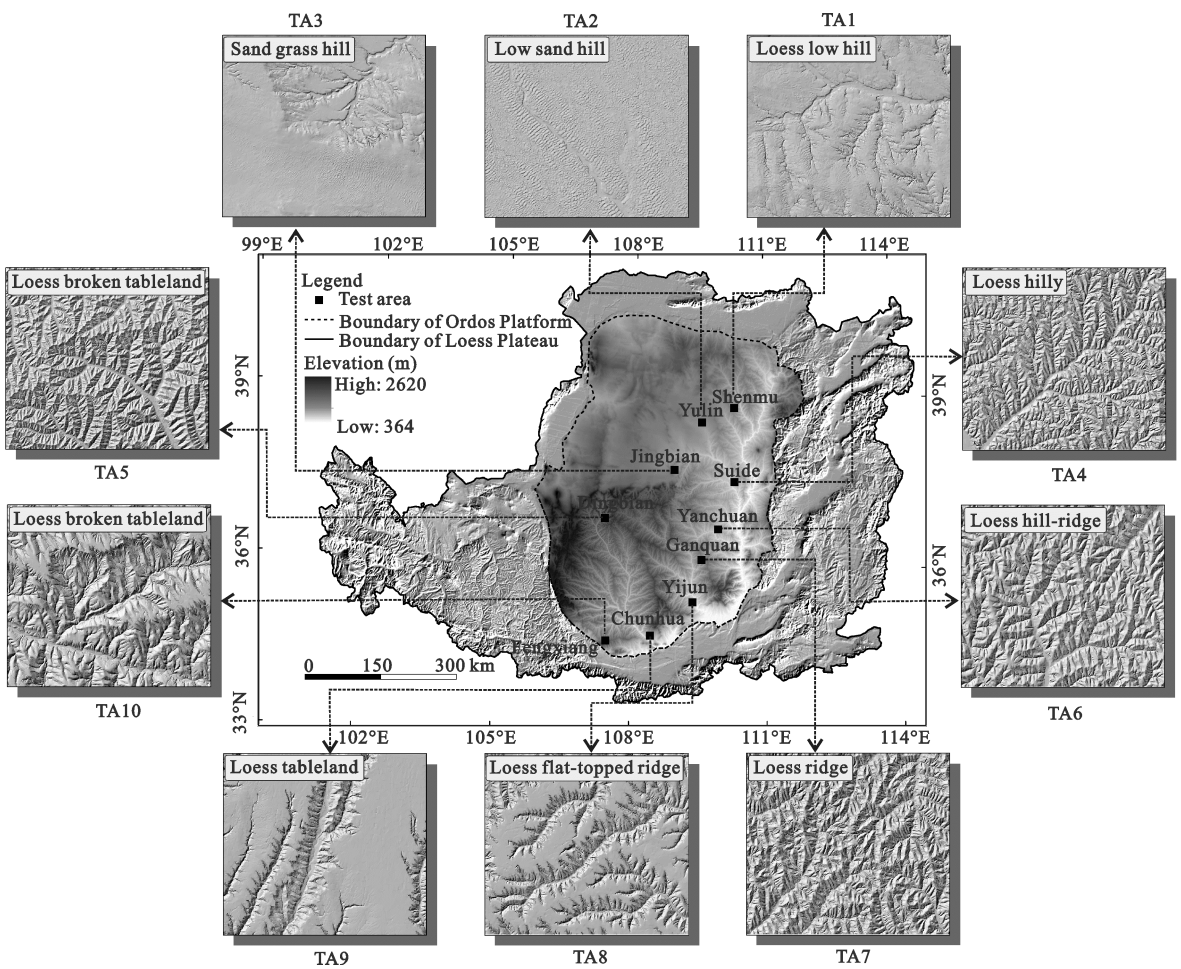

Fig. 1 Distribution of test areas in Ordos Platform. TA: test area

Table 1 A general illustration of test areas

Test area	Place name	Landform type	Rang of elevation (m)	Topographical relief (m)	Average slope gradient (°)
TA1	Shenmu	Loess low hill	1035–1322	9.47	9.23
TA2	Yulin	Low sand hill	1168–1252	3.39	7.88
TA3	Jingbian	Sand grass hill	1163–1414	6.53	6.46
TA4	Suide	Loess hilly	814–1188	33.68	29.28
TA5	Dingbian	Loess broken tableland	1307–1752	14.19	28.61
TA6	Yanchuan	Loess hill-ridge	923–1252	37.62	31.30
TA7	Ganquan	Loess ridge	1147–1459	31.39	26.74
TA8	Yijun	Loess flat-topped ridge	767–1158	22.97	19.23
TA9	Chunhua	Loess tableland	785–1175	14.62	12.33
TA10	Fengxiang	Loess broken tableland	1204–1677	9.39	29.87

Note: TA is test area

2.3 Methods

We proposed a new terrain derivative named Landform Planation Index (LPI) to describe the planation characteristics at different stages of the landform evolutionary process. The LPI is defined as the similarities between the summit surface, which is formed according to the clustering results of the peaks and the modeled critical planation surface in a certain area. The LPI could be used to describe the planation characteristics during the landform evolutionary process. The summit surface is the elevation connection of the cluster peaks extracted from DEMs. The critical planation surface is a peneplain, which could mainly be described by the critical stable area and critical slope gradient. The suitable slope gradient and the stable size of area for optimized extraction of the planation surfaces will also be discussed.

2.3.1 Experimental scheme

In order to quantitatively express the LPI, we firstly extract peaks, and then calculate LPI. The experimental scheme is shown as follows (Fig. 2).

2.3.2 Peaks extraction

A peak is the maximum elevation point in the local area, which represents the convex in all the directions. Based on the extraction method of peaks (Luo and Tang, 2010), saddles (Xiong *et al.*, 2013) and gully heads (Zhu *et al.*, 2014), this study adopted a peak extraction method based on the profile of the watershed boundary. Generally, all peaks should be located at watershed boundary (Xiong *et al.*, 2013). The elevation of these peaks is a local maximum of the watershed boundary

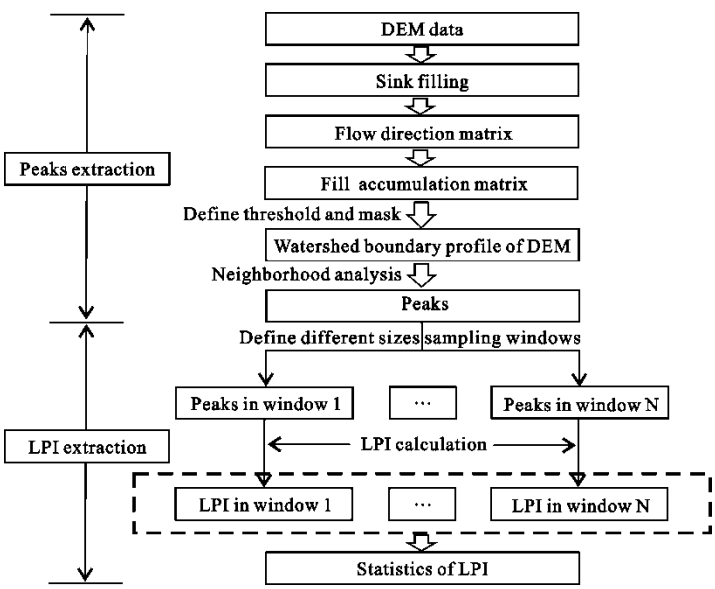

Fig. 2 Experimental scheme. DEM: Digital Elevation Model; LPI: Landform Planation Index

profile (Fig. 3). Based on the watershed boundary profile, the extraction method is carried out with neighborhood statistics operation. The specific steps are illustrated as follows.

(1) Extraction of watershed boundary line and profile. 1) Fill sinks of the original DEM data. 2) Calculate the flow direction matrix. 3) Calculate the accumulated matrix of confluence. 4) Extract the line of watershed boundary. 5) Extract the cell of original DEM data that correspond to the watershed boundary profile. A watershed boundary profile with elevation is defined as a watershed boundary profile DEM.

(2) Extraction of peaks. Neighborhood analysis in ArcGIS software is used to derive the maximum values from the watershed boundary profile of DEM. A circular neighborhood is used for the moving analysis window. To find the optimized size for the moving analysis window, radius from 3 cells to 21 cells were examined, respectively. A final maximum value of the DEM (max-DEM) is derived using the neighborhood analysis with the optimal window size of 17. After that, an overlay operation is implemented by subtracting the max-DEM with the original DEM. In the subtraction result, the raster points with values equal to zero will be marked as the peaks. At last, the raster-based results of the peaks will be converted to the vector peaks.

2.3.3 LPI calculation

To extract the LPI formed by the elevation connection of the cluster peaks (Fig. 4a), the LPI should be described mathematically.

As shown in Fig. 4b, there are a series of peaks in the circular sampling window whose center is at A and whose radius is R. Taking B for instance, calculation of the LPI (F_{AB}) between A and B is as follows:

$$F_{AB} = \Delta H_{AB} - \Delta L_{AB} \tan\alpha \quad (1)$$

where ΔH_{AB} is the elevation difference between point A and point B, ΔL_{AB} is their horizontal distance, and α is the critical slope gradient. In the circular sampling area centered at point A, there exists a number of n peaks (except A). Based on Equation (1), the calculation of the LPI (F_{AP_i}) between A and P_i ($1 \le i \le n$) is shown as follows:

$$F_{AP_i} = \Delta H_{AP_i} - \Delta L_{AP_i} \cdot \tan\alpha \quad (2)$$

where ΔH_{AP_i} is the elevation difference between point A and point P_i, ΔL_{AP_i} is their horizontal distance. Therefore, the maximum of F_{AP_i} is used as the LPI of peak A (F_A).

$$F_A = \max(F_{AP_i}) = \max(\Delta H_{AP_i} - \Delta L_{AP_i} \cdot \tan\alpha) \quad (3)$$

We suppose that if F_A is smaller or equal to 0, the circular area centered at A is flattened into a planation surface; and if F_A is larger than 0, this circular area is not a planation surface. The bigger value F_A is, the lower level flattened degree will be.

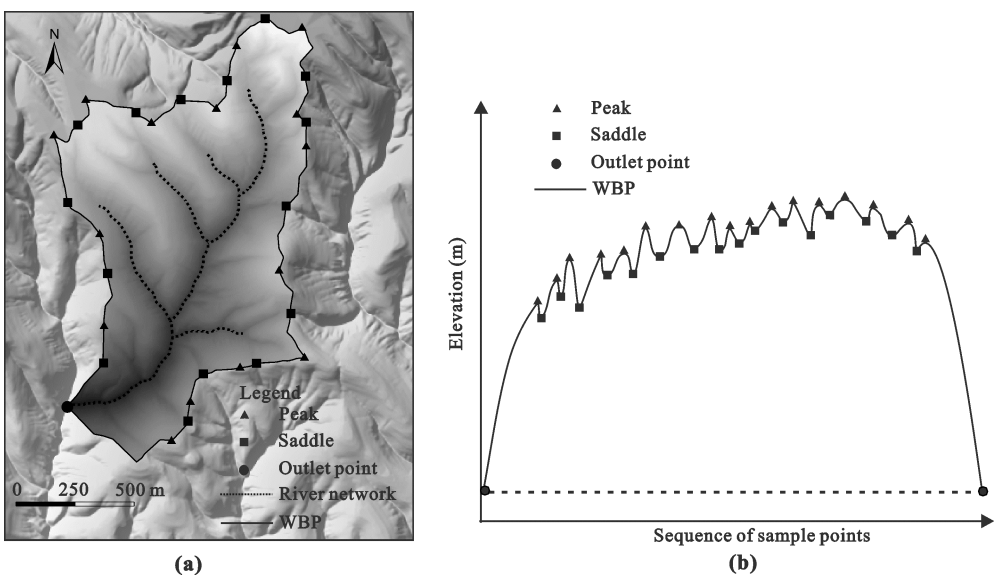

Fig. 3 Peaks distribution at a watershed (a) and morphogical parsing of watershed boudary profile (b). WBP: watershed boundary profile

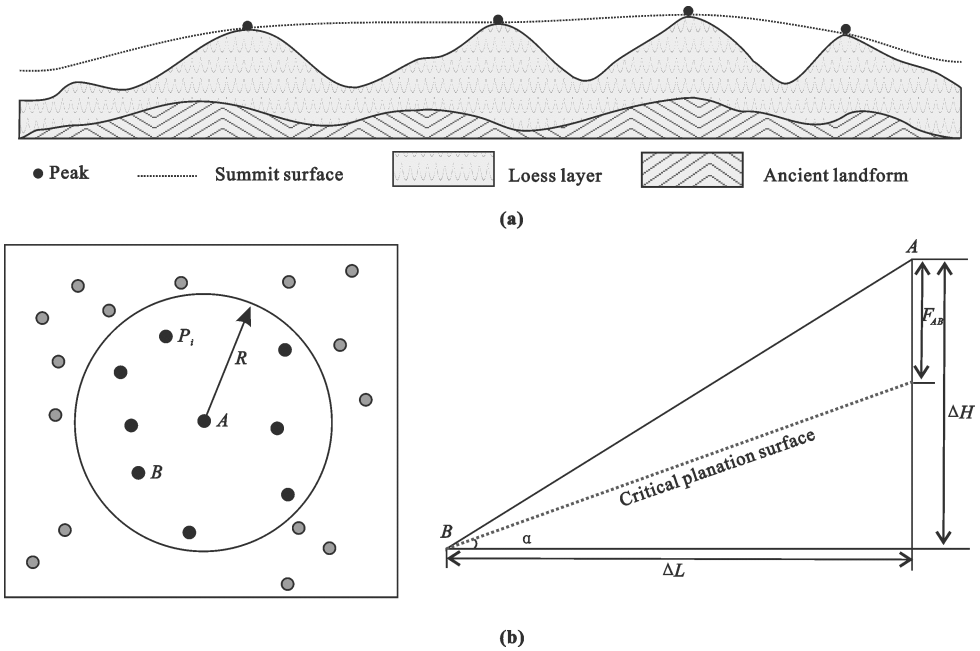

Fig. 4 Topographical profile (a) and schematic diagram of LPI (b). *A*, *B* and P_i are marked as peaks at a circular buffer centered at *A* with radius *R*; ΔH is the elevation difference between *A* and *B*; ΔL is the horizontal distance between *A* and *B*; F_{AB} is the LPI value between *A* and *B*

The procedure for extracting the LPI is as follows. 1) Create a circular buffer whose center is at a peak. The initial radius of the moving analysis window is 100 m. 2) Search over all the peaks in the buffer area, and calculate the LPI of the peak based on Equation (3). 3) Gradually expand the buffer area in increments of 50 m. The LPI value will be extracted with different radius size of the buffer area. 4) Extract the LPI of all peaks in entire test areas with different buffer areas.

3 Results and Analyses

3.1 Spatial variation of LPI in different areas

The maximum, minimum, and average value of the LPI can be used to reflect the topographic relief of the connected summit surface. While the standard deviation value of the LPI can reflect the discrete degree, which will increase with the increment of fragmentation degree. If the proportion of the LPI value less than zero, it indicates that the summit surface stay in a planation condition in the test areas; and if the proportion is close to 100%, it indicates that the entire test area is a typical planation surface.

Table 2 is the statistical results of the LPI with different attributes in the ten typical test areas. Under the controlling effects from the underlying paleotopography, the modern landforms of TA4, TA5 and TA6 were developed with high relief topographic characteristics; therefore, the maximum, minimum and average value of LPI in these areas are relatively larger. As the fragmentation degree of summit surfaces in TA5 and TA8 are larger than the values of the loess hill gully areas, the standard deviation values of TA5 and TA8 are relatively larger. On a basis of inheriting underlying low relief paleotopography, tableland surfaces exist in TA8 and TA9. What is more, there are many low-relief sand dunes exist in the test areas of TA1, TA2 and TA3; therefore, their proportions of the LPI less than zero are keeping a rather big value, some even close to 100%.

Figure 5 shows that the trend in change of maximum , average and the proportion of the LPI less than 0 in the different test areas. As shown in Figs. 5a, 5b, the low values of maximum and average results are located in northern sand hill areas and southern loess tableland areas, and their high values appear in mid hilly and gully areas. From south to north, with the change of the geomorphologic types from loess tableland, loess flat-topped ridge, loess ridge, loess hill-ridge, loess broken tableland, loess hilly to loess low hill, their statistical results increase first, and then decrease. This result indicates that a ′strong-weak-strong′ trend of topographic relief of current terrain and underlying

Table 2 Statistics of planation index with radius of 1100 m and critical slope gradient of 4°

Test area	Number of peaks	Maximum (m)	Minimum (m)	Average (m)	Standard deviation	Counts (LPI < 0)	Proportion (%)
TA1	196	2.60	–65.82	–13.83	9.83	193	98.47
TA2	1438	8.11	–27.65	–6.13	3.59	1377	95.76
TA3	424	29.91	–94.32	–18.36	13.22	406	95.75
TA4	733	79.63	–13.22	20.94	15.59	42	5.73
TA5	240	127.66	–28.07	53.90	32.48	5	2.08
TA6	351	82.11	–25.47	21.20	18.92	36	10.26
TA7	276	57.12	–24.37	6.56	13.53	91	32.97
TA8	91	55.56	–85.06	–18.83	25.56	73	80.22
TA9	57	–8.10	–98.84	–36.67	24.85	57	100.00
TA10	452	58.53	–20.22	7.95	13.68	149	32.96

Note: TA is test area; LPI is Landform Planation Index

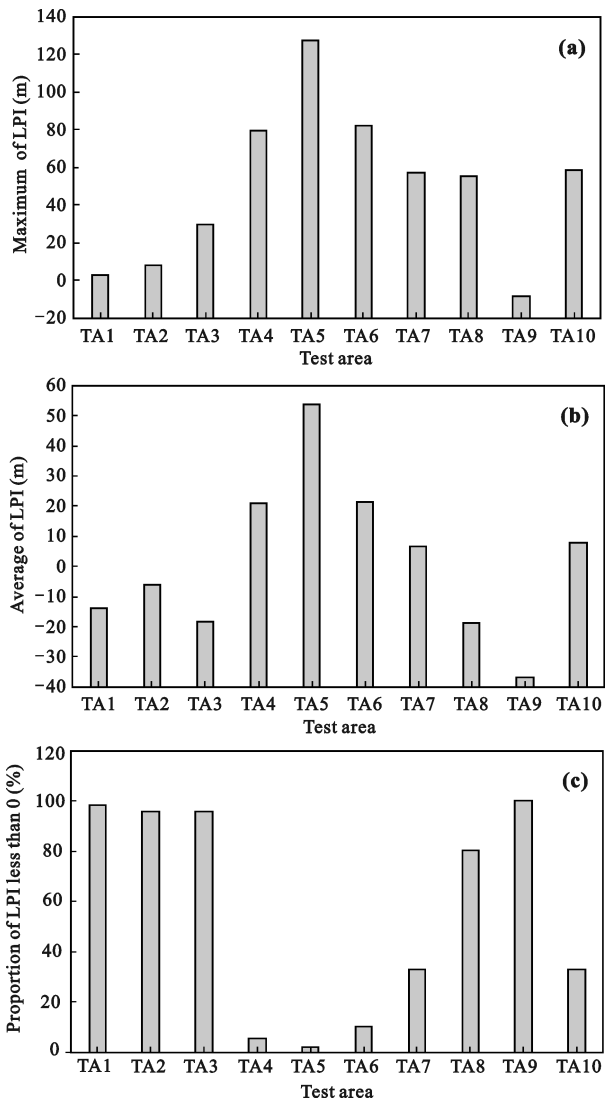

Fig. 5 Comparison of index of different test areas. (a) Maximum of LPI. (b) Average of LPI. (c) Proportion of LPI less than 0. LPI is Landform Planation Index

paleotopography from north to south. The fragmentation degree of surface in mid hilly and gully areas appear to be larger than the fragmentation degree of surface in northern loess low hill areas. In addition, the proportion of LPI less than 0 could be used to measure flatten degree in different test areas. Larger value of the LPI indicates the flatter level of the current planation surface. As shown in Fig. 5c, we can observe that the flatten degree of different landform type areas in the Loess Plateau from large to small is TA9, TA1, TA2, TA3, TA8, TA10, TA7, TA6, TA4, and TA5. The results keep in high concordance with the evolution process and planation process of loess landform.

3.2 Flatten degree of summit surface

The slope gradient among the summit surfaces can reflect the undulation, flatten degree and topographical complexity of the residual planation surfaces. As a result, on the basis of stable sampling window, we firstly extract the maximum of slope gradient of the summit surface in 10 typical test areas, and then carry out a comparison analysis of the flatten degree in every slope gradient classes.

As shown in Fig. 6, TA1, TA2, and TA9 represent loess low hill area, low sand hill area, and loess tableland area, respectively. Their high values of frequency curves are on a range from 0° to 3° and their accumulative curves reach 100% at the slope gradient of 4°. These results indicate that a gently rolling topography and a high flatten degree of residual summit surface could be found in these test areas. The TA4, TA5, and TA6 are mainly in loess hilly gully areas. Their high values of frequency curves are on a range from 6° to 7°

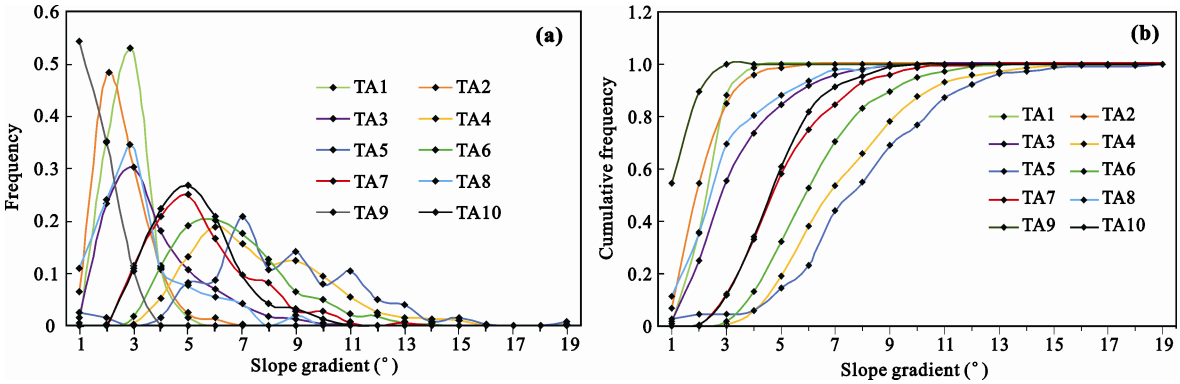

Fig. 6 Frequency (a) and cumulative frequency (b) with different slope classes

and their accumulative frequency curves reach approximately 100% at slope gradient of 15°. These results indicate that a relative broken landform with high topographical relief of summit surface and low flatten degree could be detected in these test areas. Comparing the accumulative frequency with different slope classes, we can also conclude that the flatten degree of different landform type areas in the Ordos Platform from large to small should be TA9, TA1, TA2, TA3, TA8, TA10, TA7, TA6, TA4, and TA5. This result could be used to verify the rationality of the LPI value in Fig. 5.

4 Discussion

The analysis scale (sampling window radius in this paper) and selected critical slope gradient according to the LPI algorithm would significantly affect the final results of the LPI calculated. Normally, the LPI value is getting stable after the area of sampling window reaches a rather big size. The selected critical slope gradient could directly influence the accuracy of calculation result of the LPI.

4.1 Effect of slope gradient

The slope gradient between peaks, i.e., the slope gradient between summit surfaces, is one of the critical parameters for the calculation of the LPI. In order to find a suitable critical slope gradient, this study investigated the relationship between the average value of the LPI and the different critical slope gradients. These slope gradients are ranging from 1° to 7° with the interval of 0.5°. The 7° is used as the threshold value as the slope gradient of the planation surface is always less than 7° (Goudie *et al.*, 1985; Small, 1978; Feng and Cui, 2002). As shown in Fig. 7, it shows that the average value of the LPI decreases gradually with the increase of the slope gradient. These test areas (e.g., TA1: loess low hill; TA2: low sand hill; TA3: sand grass hill; TA8: loess flat-topped ridge; TA9: loess tableland) with flat surface have relatively small average value of the LPI in different slope gradients. Moreover, the average value of the LPI in those test areas drop to negative with the raising of slope gradient. What is more, some test areas (TA4: loess hilly; TA5: loess broken tableland; TA6: loess hill-ridge; TA7: loess ridge; TA10: loess broken tableland) with high dense gullies have large average value of the LPI. For example, those test areas with rather coarse terrain, i.e., TA4 and TA5, will take a high topographical relief of summit surface, and their mean value of the LPI is over 0 in whole range of slope gradients. Especially, as to TA3, a transition part of sand dunes and loess gully from low relief to rugged terrain, its curve reaches 0 at about 4°. Therefore, 4° is taken as a suitable critical slope gradient in this study.

4.2 Effect of analysis scale

According to the aforementioned calculation method of the LPI, the search radius of sampling window is one of

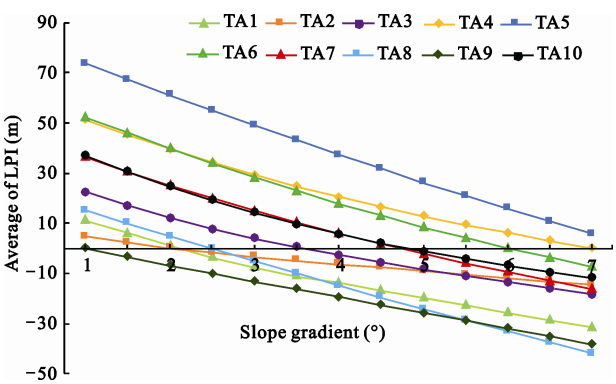

Fig. 7 A trend of maximum of LPI with increase of slope gradient

the critical parameters affecting final result. In order to keep the LPI results stable, the area of sampling window should be larger than the critical stable area in the calculation. Figure 8 shows the LPI get variable value in different test areas with different size of radius. It shows that different critical stable areas exist in different landform types. The results indicate that, with the increase of sampling window radius, the tendency of LPI increases along with the raising of radius firstly, and then keeps stable. Taking the maximum value of the LPI for example, as shown in Fig. 8, we could find the variation tendency of LPI maximum value with the increase of radius. Each test area possesses of its own critical stable area based on the turning point of the curve line. TA1, TA2 and TA9, at relatively low relief terrain area, takes rather low critical stable areas (TA1: 200 m; TA2: 400 m; TA9: 200 m). This result could find its inherent reason, namely, current terrain inherits the low relief underlying paleotopography, i.e., the morphology of peneplain. In addition, TA5 and TA6 have the relatively large stable areas (TA5: 1100 m; TA6: 1000 m). All results show that when the radius of sampling area is large than 1100 m, the maximums of the LPI in different test areas appear to be stable. Therefore, the 1100 m of sampling window radius is picked as the stable value of the LPI calculation.

5 Conclusions

In this study, the summit surfaces are formed according to the clustering results of the peak points extracted from DEMs. The summit surfaces are used to investigate the morphological characteristics of planation surfaces. The concept of Landform Planation Index (LPI) and its extraction method are introduced. (1) The LPI is a suitable index to quantify the characteristics of the planation surfaces, which could be applied to investigate the planation processes in geomorphological studies. (2) Based on the discussion of the residual summit surface of Loess Plateau and underlying bedrock terrain of Ordos Platform, 4° is determined as a critical slope gradient for a planation surface in the loess area. The stable area of the LPI increase gradually with landform complexity, and 1100 m of the stable area radius is demonstrated as the stable search radius for the calculation and analysis of the LPI. By the analysis of the LPI result, the different summit surfaces and their corresponding underlying paleotopography showed a 'strong-weak-strong' flattened degree from north to south in the Loess Plateau. The summit surfaces of loess tableland reveal a fully developed planation situation of underlying paleotopography.

This study is virtually mapping the relationship between current surface and underlying ancient planation surface. Anyway, the LPI could be found to play a part in identification and reconstruction of the real planation surface. More work should be probed into its deep inner mechanism (e.g., the variance of planation process), and summit surfaces should reflect the planation surfaces at different grade level in details. Hence, the LPI should enrich its attributes to express the multiple-stage leveled of the surfaces.

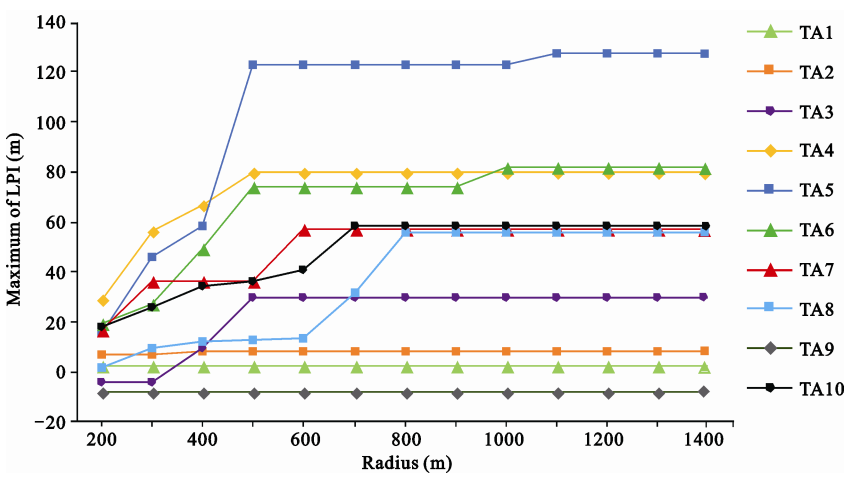

Fig. 8 A trend of maximum of LPI with increase of search radius at different test areas

Acknowledgements

ZHONG Teng from Department of urban planning and design, University of Hong Kong is appreciated for his valuable comments and discussion during the course of this work.

References

Bessin P, Guillocheau F, Robin C *et al.*, 2014. Planation surfaces of the Armorican Massif (western France): denudation chronology of a Mesozoic land surface twice exhumed in response to relative crustal movements between Iberia and Eurasia. *Geomorphology*, 233: 75–91. doi: 10.1016/j.geomorph.2014.09.026

Bi H X, Tan X Y, Li X Y, 2006. Digital terrain analysis based on DEM. *Journal of Beijing Forestry University*, 1(1): 54–58. doi: 10.1007/s11461-005-0002-4

Carbonel D, Rodríguez-Tribaldos V, Gutiérrez F *et al.*, 2015. Investigating a damaging buried sinkhole cluster in an urban area (Zaragoza City, NE Spain) integrating multiple techniques: geomorphological surveys, DInSAR, DEMs, GPR, ERT, and trenching. *Geomorphology*, 229: 3–16. doi: 10.1016/j.geomorph.2014.02.007

Coltorti M, Pieruccini P, 2000. A late lower pliocene planation surface across the italian peninsula: a key tool in neotectonic studies. *Journal of Geodynamics*, 29(3–5): 323–328. doi: 10.1016/S0264-3707(99)00049-6

Cui Z J, Gao Q Z, Liu G N *et al.*, 1996. Planation surfaces, palaeokarst and uplift of Xizang (Tibet) Plateau. *Science in China* (*Series D*), 39(4): 391–400.

Cui Z J, Gao Q Z, Liu G N, 1997. The initial elevation of palaeokarst and planation surfaces on Tibet Plateau. *Chinese Science Bulletin*, 42(11): 934–939. doi: 10.1007/BF02882552

Cui Z J, Li D W, Feng J L *et al.*, 2002. Comments on the planation surface once more. *Chinese Science Bulletin*, 47(10): 793–797. doi: 10.1360/02tb9179

Cui Z J, Li D W, Wu Y Q *et al.*, 1999. Comment on planation surface. *Chinese Science Bulletin*, 44(22): 2017–2022. doi: 10.11821/dlxb201409006

Dinesh S, 2007. The effect of morphological smoothening by reconstruction on the extraction of peaks and pits from digital elevation models. *Pattern Recognition Letters*, 28(12): 1400–1406. doi: 10.1016/j.patrec.2007.02.011

Dennis R L, 2004. Landform resources for territorial nettle-feeding Nymphalid butterflies: biases at different spatial scales. *Animal Biodiversity and Conservation*, 27(2): 37–45.

Dong W J, Tang M C, 1997. A numerical modelling study on the processes of uplift and planation of the Tibetan Plateau. *Science in China* (*Series D*), 40(3): 246–252.

Evans I S, 1972. General geomorphometry, derivatives of altitude, and descriptive statistics. In: Chorley R J *et al*. (eds). *Spatial Analysis in Geomorphology*. London: Harper & Rows Press, 17–90.

Feng J L, Cui Z J, 2002. The reconstruction of fossil planation surface in China. *Chinese Science Bulletin*, 47(5): 434–440. doi: 10.1360/02tb9101

Goudie A, Atkinson B W, Gregory K J *et al.*, 1985. *The Encyclopaedic Dictionary of Physical Geography*. Oxford: Basil Blackwell Ltd., 118–121, 165, 325–336.

Grohmann C, Miliaresis G, 2013. Geological applications of digital terrain analysis. *International Journal of Geographical Information Science*, 27(7): 1403–1404. doi: 10.1080/13658816.2013.772617

Haider V L，Jan K, István D *et al.*, 2015. Identification of peneplains by multi-parameter assessment of digital elevation models. *Earth Surface Processes & Landforms*, 40(11): 1477–1492. doi: 10.1002/esp.3729

Hara Y, Thaitakoo D, Takeuchi K, 2008. Landform transformation on the urban fringe of Bangkok: the need to review land-use planning processes with consideration of the flow of fill materials to developing areas. *Landscape & Urban Planning*, 84(1): 74–91. doi: 10.1016/j.landurbplan.2007.06.009

Johansson M, 1999. Analysis of digital elevation data for palaeosurfaces in south-western Sweden. *Geomorphology*, 26(4): 279–295. doi: 10.1016/S0169-555X(98)00068-3

Li H, Huang X Y, Deng Q L *et al.*, 2012. Mapping of planation surfaces in the southwest region of Hubei Province, China: using the DEM-Derived painted relief model. *Journal of Earth Science*, 23(5): 719–730. doi: 10.1007/s12583-012-0290-1

Li J J, Fang X M, 1999. Uplift of the Tibetan Plateau and environmental changes. *Chinese Science Bulletin*, 44(23): 2117–2124. doi: 10.1007/BF03182692

Li J J, Fang X M, Ma H Z *et al.*, 1996. Geomorphological and environmental evolution in the upper reaches of the Yellow River during the late Cenozoic. *Science in China* (*Series D*), 39(4): 380–390.

Liu Y, Wang Y X, Pan B T, 1999. A preliminary approach on the 3D presentation and quantitative analysis of planation surface. *Geographical Research*, 18(4): 391–399. doi: 10.11821/yj1999040009

Lu Guonian, Qian Yadong, Chen Zhongming, 1998. Study of automated extraction of shoulder line of valley from grid digital elevation data. *Scientia Geographica Sinica*, 18(6): 567–573. (in Chinese)

Luo Mingliang, Tang Guoan, 2010. Mountain peaks extraction based on geomorphology cognitive and space segmentation. *Science of Surveying & Mapping*, 35(5): 126–128. (in Chinese)

Nash C R, 1988. Delineation of structurally controlled landforms in southeastern Queensland using remotely sensed data. *Earth-Science Reviews*, 25(5–6): 427–432. doi: 10.1016/0012-8252(88)90009-8

Poulos S E, Gaki-Papanastasiou K, Gialouris P *et al.*, 2012. A geomorphological investigation of the formation and evolution of the Kaiafas sand-dune field (Kyparissiakos Gulf, Ionian Sea, eastern Mediterranean) in the Late Holocene. *Environmental Earth Sciences*, 66(3): 955–966. doi: 10.1007/s12665-011-1305-4

Rigol-Sanchez J P, Stuart N, Pulido-Bosch A, 2015. ArcGeomor-

phometry: a toolbox for geomorphometric characterization of DEMs in the ArcGIS environment. *Computers & Geosciences*, 85: 155–163. doi: 10.1016/j.cageo.2015.09.020

Römer W, 2010. Multiple planation surfaces in basement regions: implications for the reconstruction of periods of denudation and uplift in southern Zimbabwe. *Geomorphology*, 114(3): 199–212. doi: 10.1016/j.geomorph.2009.07.001

Small R J, 1978. *The Study of Landforms* (*Second Edition*). London: Cambridge University Press, 154–327.

Tang Guoan, 2014. Progress of DEM and digital terrain analysis in China. *Acta Geographica Sinica*, 69(9): 1305–1325. (in Chinese)

Thorne C R, 1998. Stream reconnaissance handbook: geomorphological investigation and analysisanalysis of river channels. *Stream Reconnaissance Handbook Geomorphological Investigation & Analysis of River Channels*, 31(2): 186–187.

Veldkamp A, Dijke J J V, 2000. Simulating internal and external controls on fluvial terrace stratigraphy: a qualitative comparison with the Maas record. *Geomorphology*, 33(3): 225–236. doi: 10.1016/S0169- 555X(99)00125-7

Wang X Y, Lu H, Vandenberghe J *et al*., 2012. Late Miocene uplift of the NE Tibetan Plateau inferred from basin filling, planation and fluvial terraces in the Huang Shui catchment. *Global & Planetary Change*, 88–89(2): 10–19. doi: 10.1016/j.gloplacha. 2012.02.009

Wu Hailuo, Chen Luanlin, 2013. Research on the information extraction yuntai mountain planation surface based on the data of DEM. *Territory & National Resources Study*, (5): 26–27. (in Chinese)

Xiong Liyang, Tang Guoan, Yan Shijiang, 2013. Grading extraction method of saddles based on DEM. *Science of Surveying and Mapping*, 38(2): 181–183. (in Chinese)

Xiong L Y, Tang G A, Yuan B Y *et al*., 2014a. Geomorphological inheritance for loess landform evolution in a severe soil erosion region of Loess Plateau of China based on digital elevation models. *Science China Earth Sciences*, 57(8): 1944–1952. doi: 10.1007/s11430-014-4833-4

Xiong L Y, Tang G A, Li F Y *et al.*, 2014b. Modeling the evolution of loess-covered landforms in the Loess Plateau of China using a DEM of underground bedrock surface. *Geomorphology*, 209: 18–26. doi: 10.1016/j.geomorph.2013.12.009

Xiong L Y, Tang G A, Strobl J *et al*., 2015. Paleotopographic controls on loess deposition in the Loess Plateau of China. *Earth Surface Processes and Landforms*, in press. doi: 10. 1002/esp.3883

Yi H S, Wang C, Liu S *et al.*, 2000. Sedimentary record of the planation surface in the Hoh Xil Region of the northern Tibet Plateau. *Acta Geologica Sinica*, 74(4): 827–835. doi: 10.3321/j. issn:1000-9515.2000.04.010

Zhang K, 2008. Planation surfaces in China: one hundred years of investigation. In: Grapes R H *et al.* (eds.). *History of Geomorphology and Quaternary Geology*. London: Geological Society London Special Publications, 171–178.

Zhang Ke, Huang Yukun, 1995. Researches on the planation surfaces in north Guangdong. *Tropical geography*, 15(4): 295–305. (in Chinese)

Zhu Hongchun, Tang Guoan, Qian Kejian *et al*., 2014. Extraction and analysis of gully head of Loess Plateau in China based on digital elevation model. *Chinese Geographical Science*, 24(3): 328–338. doi: 10.1007/s11769-014-0663-8